The Adequacy and Compatibility of Compartmental Models of Electrolyte Exchange in the Dog's Heart

G. ARTURSON,[1] T. GROTH,[2] G. GROTTE,[3] P. MALMBERG,[4]
R. SAMUELSSON[5] and U. SJÖSTRAND[5]

From the [1]Burn Center, the [3]Department of Pediatric Surgery, the [4]Department of Clinical Physiology, University Hospital; the [2]Uppsala University Data Center and the [5]Department of Physiology and Medical Biophysics, Uppsala University, Uppsala, Sweden

ABSTRACT

The exchange of electrolytes (Na, K, SO_4) and albumin in the dog's heart was studied by using tracer technique in a modified heart-lung preparation. The data were analysed in order to investigate if the system could be characterized kinetically in terms of a few distinct compartments, and to what extent tracer measurements in systemic plasma and cardiac lymph provide information about the capillary and cellular exchange of electrolytes in the dog's heart. The compartmental models used for sodium and potassium were easily conformed so as to be compatible with the tracer data and it was also possible to make them consistent with independent relevant data from the literature. However, it was not possible to construct adequate models in the sense that the model parameters were well determined by the data. This was not due to inaccurate data but to the insufficiency of this type of data to identify adequate models of the required complexity. Therefore, detailed quantitative information on the electrolyte transport across cellular membranes cannot be obtained in experimental studies of the type presented in this investigation.

The excitability of the heart muscle is heavily dependent on the extra- and intracellular concentrations of sodium and potassium ions. Analysis of the relations between changes of these concentrations and the corresponding changes of excitability and contractility would be considerably simplified if the heart could be characterized kinetically in terms of a few distinct exchanging compartments. This type of description necessarily involves simplifying assumptions concerning the number and interconnections of compartments, the relation of measurements in the body fluids to compartments etc., assumptions which limit the possibilities of drawing detailed conclusions. However, models of this kind provide simple concepts, which may be used for the description of the essential features of the system studied.

For the complete identification of a multicompartment system, it is necessary to have data from each compartment (27). This condition is often not fulfilled, which means that some aspects of the model will be less well determined. It is therefore of primary importance to test a proposed model not only for compatibility with the experimental data available, but also for the more strict condition of adequacy, which besides compatibility, requires that the parameters of the model are well determined by the data.

Compartmental analysis has been used in previous investigations of electrolyte transport in the dog's heart. Transcellular sodium and potassium exchange have been calculated and correlated to changes of cardiac frequency (8, 9, 16, 29). However, the models used in these studies were not tested for adequacy, a circumstance which limits the reliability of the results.

In the present communication, the experimental data were gathered from a simultaneous study of ^{24}Na, ^{42}K, ^{131}I-albumin and $^{35}SO_4$ in systemic plasma and heart lymph. The compartmental analysis was performed, with due consideration to the requirement of model adequacy, in order to investigate to what extent this type of data provide information about capillary and cellular exchange of electrolytes in the dog's heart.

MATERIAL AND EXPERIMENTAL PROCEDURE

The experiments were performed on modified heart-lung preparations (HLP), prepared according to Areskog (1), in four young, anaesthetized Vorsteh dogs, weighing about 20 kg. Nembutal® (30 mg/kg) was used as the anaesthetic agent. The fall in body temperature during the experiment was diminished by heating the operation table, irradiating the dog with a heat lamp and regulating the temperature of the reservoir and tubing system in the HLP. Evaporation from the open thorax was diminished by means of a plastic foil cover and the HLP was continuously supplied with 5.5 %
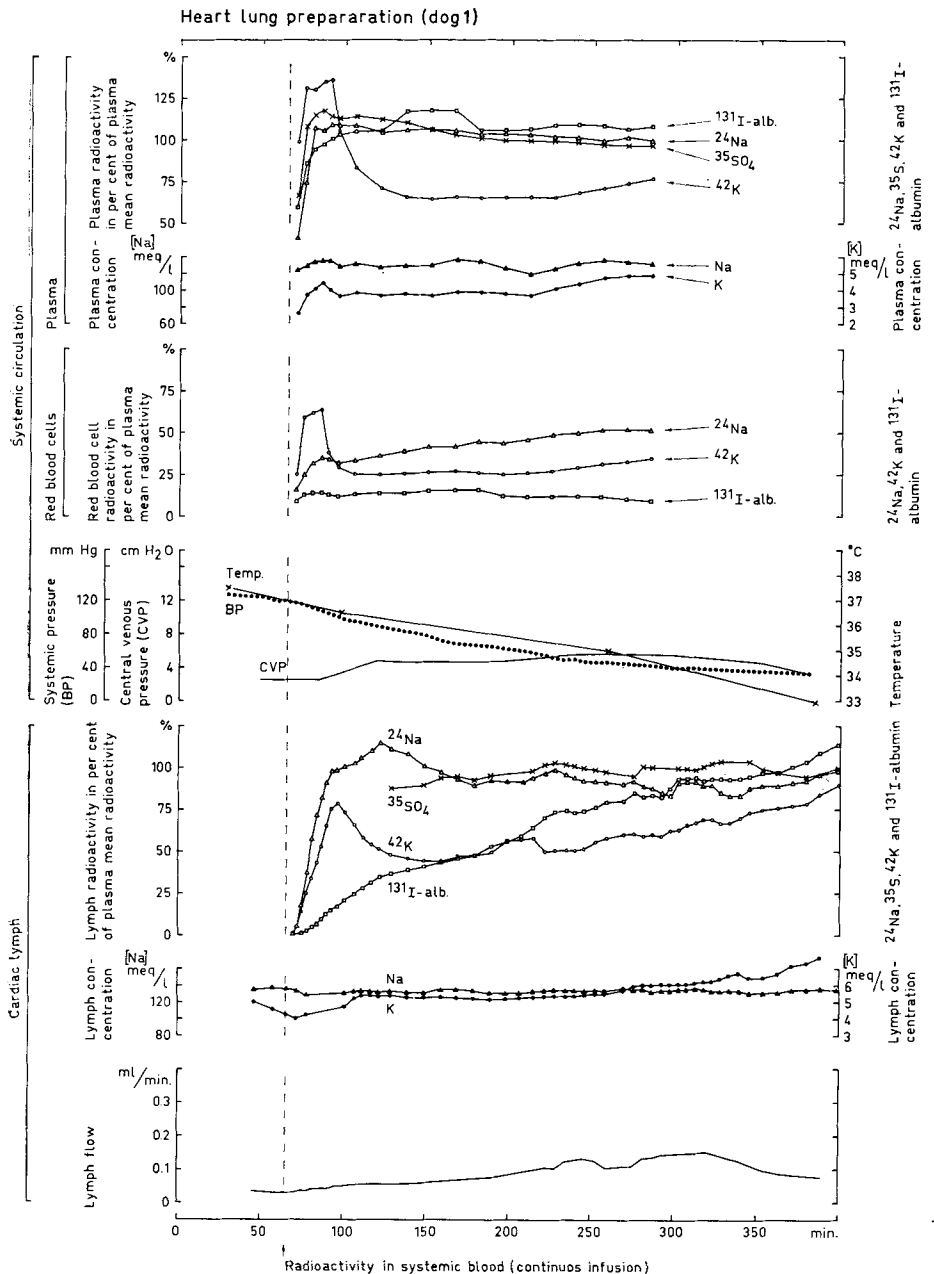
Fig. 1. Experimental results for dog 1.

glucose solution (1 ml/min), which was added to the reservoir. The heart rate (HR), the arterial systemic pressure (BP), the central venous pressure (CVP) and the temperature of the venous blood were measured. The cardiac output was measured continuously by means of an ultrasonic detector located on the tubing on the arterial side.

The tracers ^{24}Na, ^{42}K, ^{35}SO$_4$ and ^{131}I-albumin were added simultaneously to the blood reservoir. The ^{131}I-albumin had

been separated one hour previously, according to the method of Bill et al. (6), in order to remove free ^{131}I. ^{35}SO$_4$ and ^{131}I-albumin were given as a single injection. Together with the initial addition of ^{24}Na and ^{42}K, continuous infusions of these isotopes were started in order to keep the systemic plasma concentration as constant as possible. Cardiac lymph was collected in heparinized plastic tubes as described previously (2). Blood samples were taken from the reservoir and
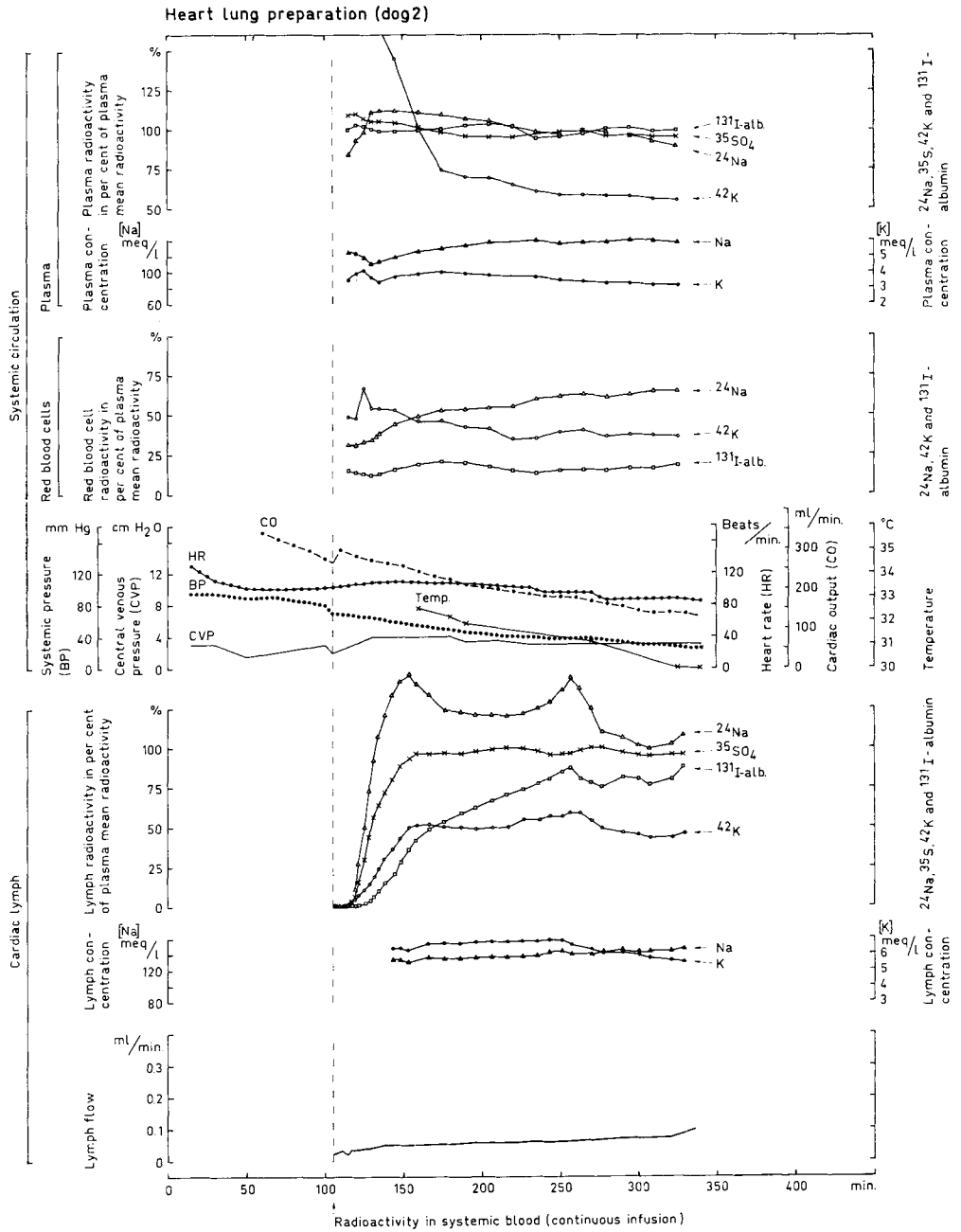
Fig. 2. Experimental results for dog 2.

were centrifuged immediately in order to separate the plasma and the red blood cells. The experiments were discontinued when the systolic systemic pressure fell below 40 mmHg.

The concentrations of sodium and potassium in cardiac lymph and systemic blood plasma were determined with an Eppendorf flame photometer. The activities of ^{24}Na, ^{42}K and ^{131}I-albumin in systemic plasma, red blood cells and cardiac ymph were measured by a gamma spectrometer (cf. 26).

^{35}SO$_4$ in the systemic plasma and the cardiac lymph was measured in a Beckman CPM-200 scintillation counter (cf. 18) after the separation of ^{35}SO$_4$ from the haemoglobin in a Sephadex® C-50 column (cf. 19).

The mean plasma concentration of the various isotopes was calculated as the mean of the values in all samples of systemic plasma and the separate concentrations (per cent) in the plasma, red blood cells and lymph samples were related

to this mean concentration. In Figs. 1, 2 and 4 the radioactive data are calculated as successive means of three consecutive measurements. The magnitudes of the errors in the experimental data were estimated from the errors of the radioactive measurements and the errors in the weighing procedures (cf. 26). During the first 15–20 min of the experimental period the errors were calculated to be about ±5% (S.D.) or even slightly larger, whereafter they decreased.

EXPERIMENTAL RESULTS

The experimental results from two dogs are presented in Figs. 1 and 2. The results from the other two dogs have been given in a previous communication (3).

The cardiac output and the arterial blood pressure gradually decreased, whereas the central venous pressure was fairly constant in the range of 0–10 cm H_2O during the experiments. The heart rate decreased somewhat, probably due to a slight decrease in body temperature during the experimental period. The lymph flow rate usually increased at the end of the experimental period. The Na and K concentrations in the systemic plasma and the lymph were practically constant throughout the experiments. These results indicate that the ionic fluxes in the heart muscle could be considered to be in steady state.

For unknown reasons, in one dog the activity of [24]Na in the cardiac lymph increased to values exceeding that of the systemic plasma (Fig. 2). These data were therefore excluded from the subsequent computational analyses.

As can be seen in Figs. 1 and 2, the [42]K and ^{131}I-albumin activities were fairly constant in the red blood cells throughout the experiments, whereas the [24]Na activity gradually increased. The initially high relative activity of the isotopes [24]Na, [42]K and ^{131}I-albumin in the packed red blood cells may be explained by an unavoidable amount of trapped plasma. The red blood cell compartment was considered to be in negligibly slow exchange with plasma and was therefore not taken into account during the subsequent compartmental analysis.

THEORY AND COMPUTATIONAL METHODS

Various types of compartmental models have been used (cf. Fig. 3), all of which are based on the assumption of a steady state, i.e. that the compartments are constant in time with respect to composition and volume. Furthermore, the resistance to tracer flow

is localized in the interface between the compartments and the mixing of tracer is assumed to be very rapid within each compartment. The flux of tracer from one compartment to another is taken as being proportional to the concentration of tracer in the compartment which the tracer is leaving. Thus the rate constants are lumped parameters, including the exchange of tracer by way of bulk flow, diffusion and other possible transport processes which can be described in this way. The various mechanisms of the transport of substances cannot therefore be resolved in this kind of analysis.

The physical models generate kinetic equations, forming a system of linear differential equations of the first order. The equations are formulated in terms of the concentration of tracer C_i (counts min^{-1} g^{-1}) in the various compartments (i) of volume V_i (ml) and the rate constants k_{ij} (min^{-1}), describing the transport of substance from compartment j to compartment i. The system of equations was integrated numerically by the use of a fourth-order Runge-Kutta method (see e.g. (5)). This approach has the apparent advantage over analytical methods (see 8) that cases with arbitrary plasma functions can be analysed, and not only cases in which the plasma concentration is constant with respect to time. The parameters (rate constants k_{ij} and volume ratios V_i/V_j) were estimated by conforming the models in a least-squares sense to the experimental tracer-concentration data from plasma and lymph samples, using a method due to Powell (22).

The models were tested for compatibility with the tracer data, and the parameter estimates and the quantities derived from them were also tested for consistency with available independent information about the biological system studied. However, the aim of the analysis was not only to find models which were *compatible* with the experimental data but rather to define *adequate* models for the description of the transport of the various substances, i.e. to find compartmental models of minimal complexity, which, besides compatibility, also define parameters which are reliably determined by the data. The estimation situation was investigated by drawing likelihood contours. The region enclosed by the sum-of-squares contour $S = S(\theta)$

$$S(\theta) \leqslant S(\hat{\theta}) \left\{ 1 + \frac{p}{n-p} F_\alpha(p, n-p) \right\}$$

where $\hat{\theta}$ is the best estimate of the parameters θ, gives an approximate $100(1-\alpha)$% confidence region,

Compartmental Models

1 = Functional plasma compartment
2 = Functional interstitial compartment
3 = Functional lymph compartment
4 = Functional intracellular compartment I or
    Functional interstitial compartment II
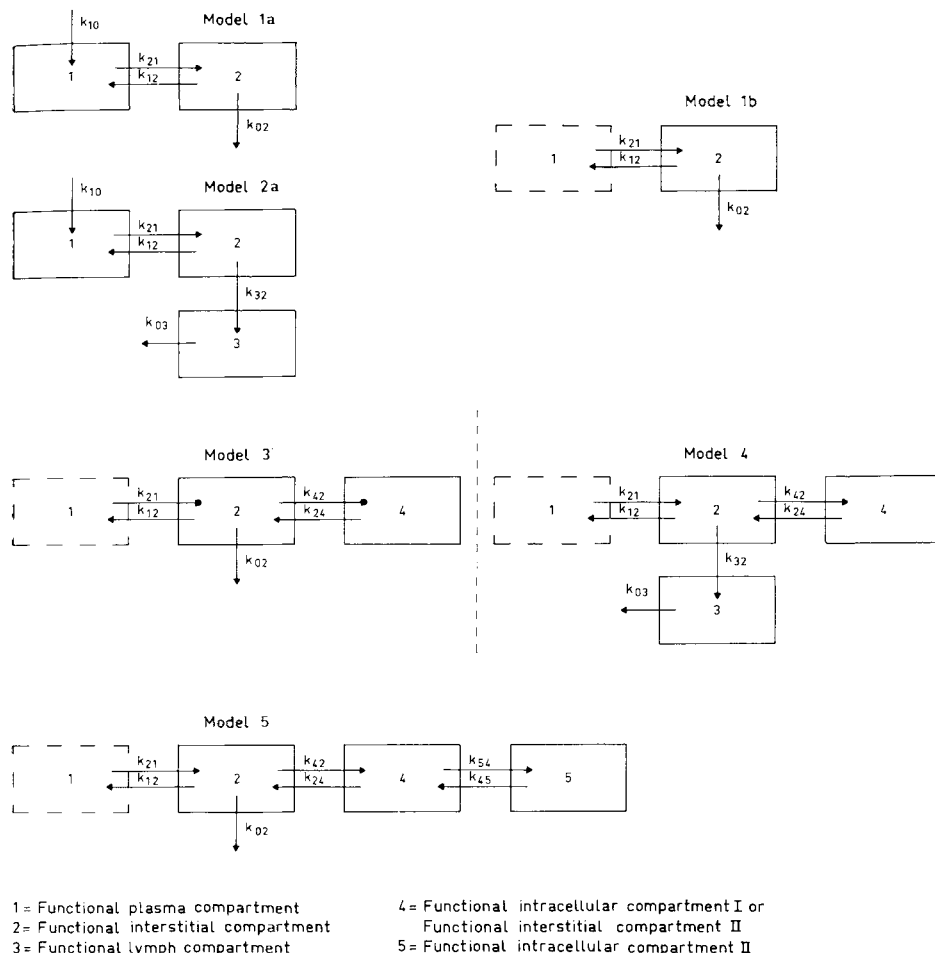5 = Functional intracellular compartment II

Fig. 3. Compartmental models used in the analysis.

if the model is reasonably linear in θ within the region of interest (4, 7).

$F_\alpha(p, n-p)$ is the α significance level of the F distribution with p and $n-p$ degrees of freedom (p=number of parameters, n=number of data points).

MODEL APPROACHES AND RESULTS

[131]I-albumin

As ^{131}I-albumin can be regarded as having a purely extracellular distribution (14), the ^{131}I-albumin tracer data were analysed in terms of an open two-compartment model (model 1a in Fig. 3). The plasma compartment was not regarded as infinite

and the concentrating effect on the tracer due to evaporation during the experiment was simulated by an equivalent inflow (k_{10}) of tracer to this compartment.

The kinetic equations for model 1a are

$$\frac{dC_1^*}{dt} = -k_{21} C_1^* + k_{12} \frac{V_2}{V_1} C_2^* + k_{10} C_1^* \tag{1}$$

and

$$\frac{dC_2^*}{dt} = (k_{12} + k_{02}) C_2^* + k_{21} \frac{V_1}{V_2} C_1^* \tag{2}$$

The parameters k_{21}, k_{12}, k_{02} and V_2/V_1 were estimated from the experimental plasma and lymph-tracer data (representing the plasma and interstitial
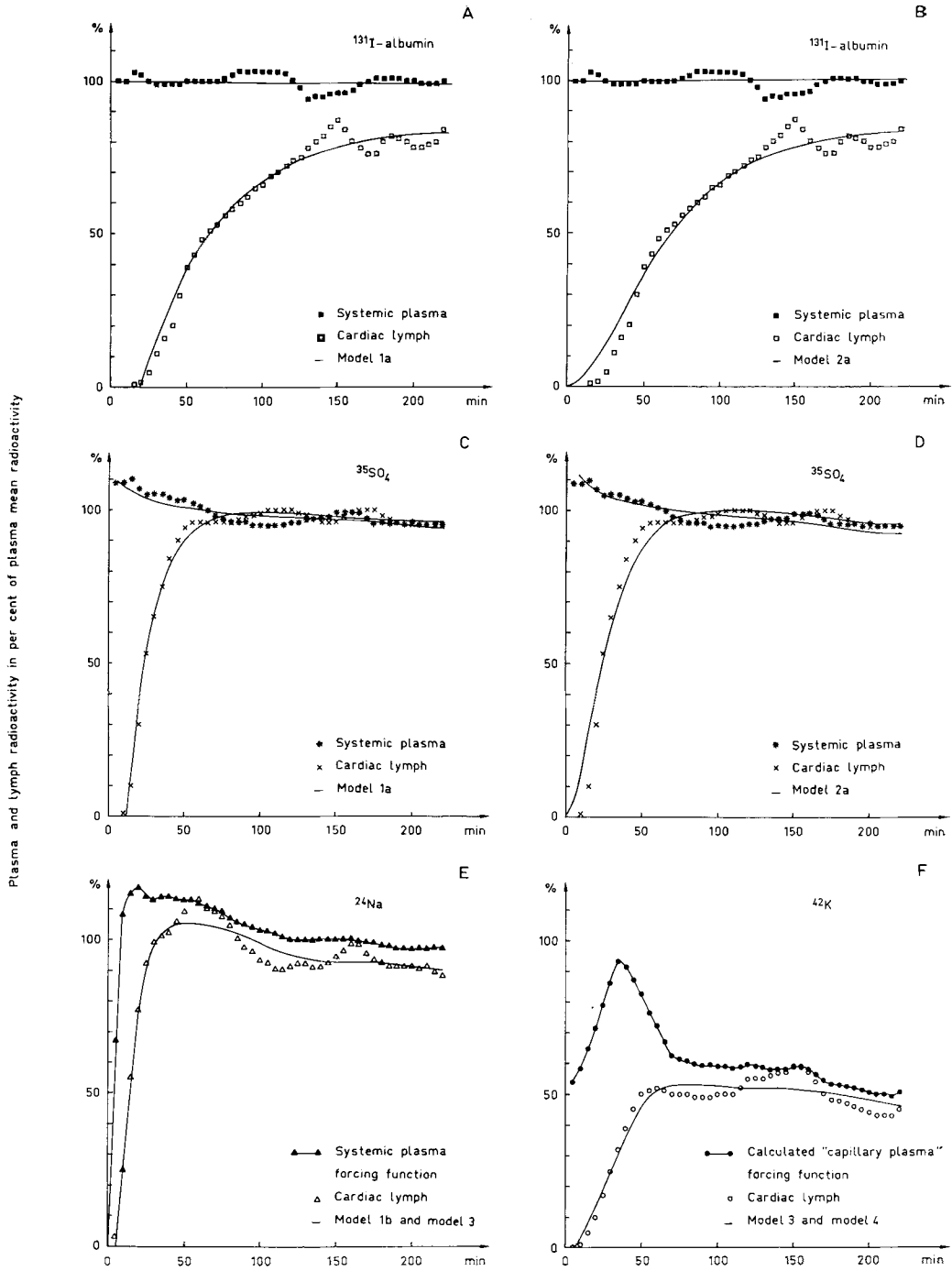
Fig. 4. Illustration of the results of conforming various models to the experimental data. Figs. A–D and F refer to dog 2 and Fig. E to dog 1.
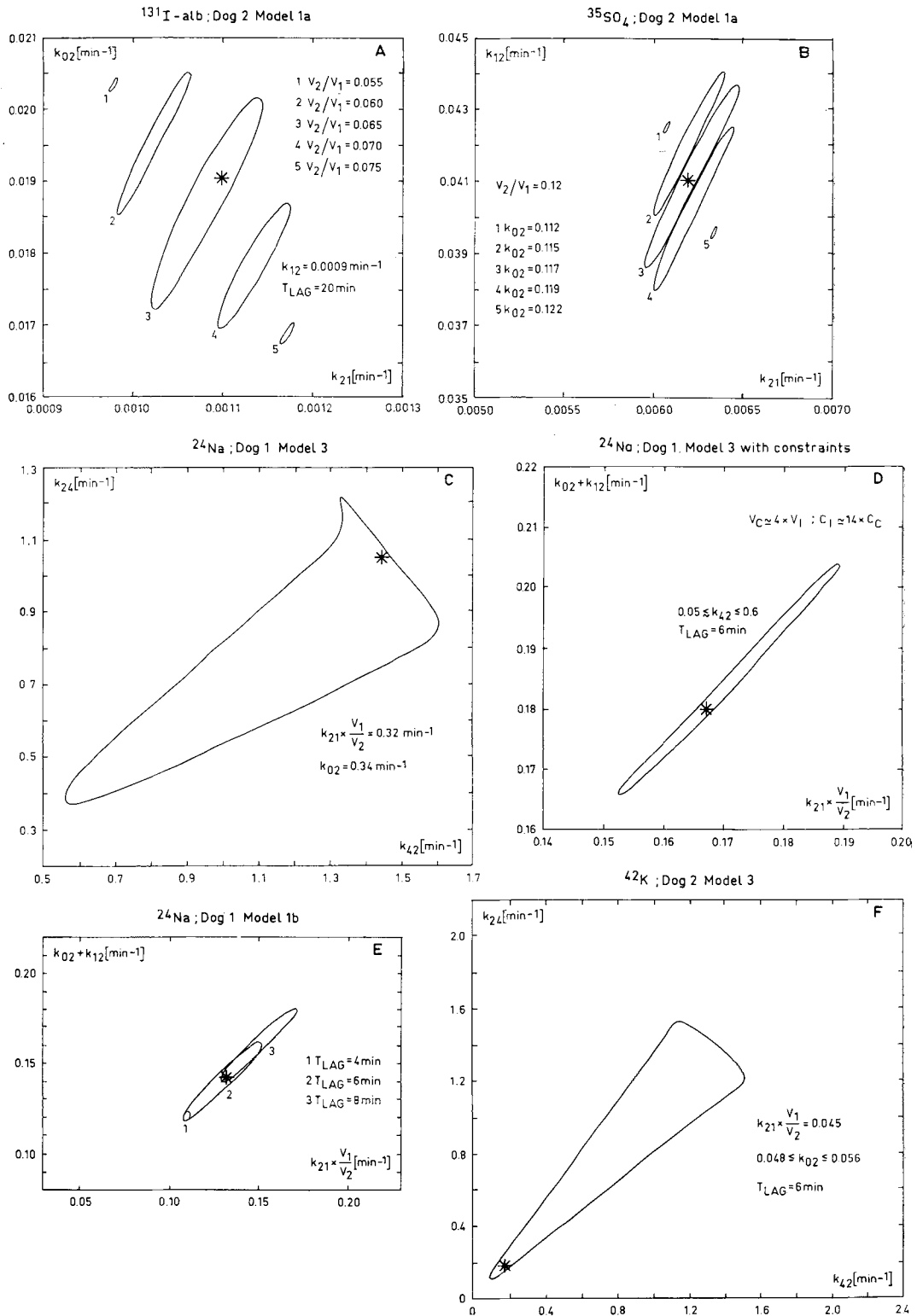
Fig. 5 Illustration of the multi-dimensional, 95 % confidence regions for the estimated model parameters by representative cross-sections.

Table I. *Parameter estimates for* [131]*I-albumin using model 1a and model 2a (dog 2) in the analysis of dogs 1, 2, 3 and 4*

Parameters	Dog 1 Model 1a	Dog 2 Model 1a	Dog 2 Model 2a	Dog 3 Model 1a	Dog 4 Model 1a	Dog 2[a] Model 1a
k_{10} (min^{-1})	0	0.0010	0.0010	0	0	0
k_{21} (min^{-1})	0.0001	0.0011	0.0010	0.0001	0.0008	0.0002
k_{12} (min^{-1})	0	0.0009	0.0043	0	0	0
k_{02}(min^{-1})	0.003	0.019	—	0.005	0.018	0.017
k_{32} (min^{-1})	—	—	0.028	—	—	—
k_{03} (min^{-1})	—	—	0.030	—	—	—
T_{LAG} (min)	2	20	0	7	26	20
V_2/V_1	0.019	0.065	0.044	0.016	0.050	0.014
V_2/V_3	—	—	1.21	—	—	—
Derived quantities						
C_P/C_I	0.6	1.2 ± 0.2	1.0	0.9	1.1	1.2

[a] Not corrected for evaporation, $k_{10} = 0$.

compartments). The influence of evaporation and other factors on the size of the plasma pool was estimated from data for stable sodium in plasma. In one dog (dog 2) there was a systematic decrease in the plasma-pool size, which was corrected for by a constant inflow of tracer ($k_{10} = 0.001$ min^{-1}); in the other dogs, the estimated pool size fluctuated irregularly but was regarded as approximately constant for the analysis (cf. k_{10} in Table I and the comments below). In order to get a good fit in the interstitial compartment, it was also necessary to introduce a time-lag parameter, T_{LAG}. T_{LAG} was chosen from the experimental data by visual extrapolation. Curvilinear interpolation of adjacent lymph values was used to calculate lymph values at times corresponding to the plasma-sample times. The parameter estimates are given in Table I and the corresponding simulated curves for dog 2 are shown in Fig. 4A, compared with the experimental data. Despite the fact that the deviations in some regions are greater than the analytical errors (see page 172), model 1a was accepted as a satisfactory description of the data, in view of the combined effects of biologically but mainly methodologically uncontrollable errors. The parameter confidence for model 1a and dog 2 is illustrated in Fig. 5A.

An alternative model (model 2a in Fig. 3) was used in an attempt to describe the data by the introduction of a special lymph compartment connected to the interstitial compartment, instead of

the time-lag parameter of model 1a. The kinetic equations for this model are:

$$\frac{dC_1^*}{dt} = -k_{21}\, C_1^* + k_{12}\, \frac{V_2}{V_1}\, C_2^* + k_{10}\, C_1^* \tag{3}$$

$$\frac{dC_2^*}{dt} = -(k_{12} + k_{32})\, C_2^* + k_{21}\frac{V_1}{V_2}\, C_1^* \tag{4}$$

and

$$\frac{dC_3^*}{dt} = -k_{03}\, C_3^* + k_{32}\, \frac{V_2}{V_3}\, C_2^* \tag{5}$$

Only dog 2, which was judged to be the best experiment, was analysed by this model and the parameters k_{21}, k_{12}, k_{32}, k_{03} and V_2/V_1 were estimated from a least-squares fit of compartments 1 and 3 to the experimental plasma- and lymph-tracer data. By introducing the plausible but still questionable constraint $C_2^*(t) \sim C_3^*(t)$, $t \geqslant 0$, it was also possible to estimate V_2/V_1 and V_2/V_3 separately. The goodness of fit is illustrated in Fig. 4B (dog 2) and the least-squares estimates of the parameters are given in Table I. As can be seen from Fig. 4B, there is a need for still more complex models in order to describe the experimental data within the limits of the analytical errors, for example, by adding a series of small compartments to explain the time lag. However, this work did not seem justified in view of the available data, as the time lag must be strongly influenced by the drainage of cardiac lymph.

From the parameter estimates in Table I, it follows, by the use of equations for mass transport and the steady-state assumption, that the concentration of unlabelled substance is the same in the plasma (C_p) and the interstitial (C_I) compartments. The amount of albumin brought back to the plasma per minute (influx rate) is of the order of 4–7% of the amount transported from the plasma per minute (efflux rate), as calculated for dog 2. These conclusions are not critically dependent on the choice of model 1a or 2a for this case. The correction for evaporation in dog 2 is, however, rather critical for the estimation of the parameters k_{21} and V_2/V_1, as can be seen in the last column of Table I. This effect may be the explanation of the discrepancies between dog 2 and dogs 1, 3 and 4 concerning V_p, and this is also the reason for the choice of dog 2 as the best experiment.

[35]SO_4

In accordance with studies of the distribution of various ions and carbohydrate molecules in the

Table II. *Parameter estimates for $^{35}SO_4$ using model 1a and model 2a (dog 2) in the analysis of dogs 2, 3 and 4*

| Parameters | Dog 2 | | Dog 3 | Dog 4 |
	Model 1a	Model 2a	Model 1a	Model 1a
k_{10} (min^{-1})	0.0010	0.0010	0	0
k_{21} (min^{-1})	0.0062	0.0085	0.0035	0.0010
k_{12} (min^{-1})	0.041	0.047	0.043	0.006
k_{02} (min^{-1})	0.012	—	0.024	0.052
k_{32} (min^{-1})	—	0.011	—	—
k_{03} (min^{-1})	—	0.066	—	—
V_2/V_1	0.12	0.15	0.05	0.02
V_2/V_3	—	6.25	—	—
T_{LAG} (min)	12	—	3	13
Derived quantities				
C_P/C_I	1.0	0.8	1.0	1.2

mammalian heart by Page & Solomon (21) and Page (20), and in the frog heart by Danielson (10), SO_4 can be regarded as having a purely extracellular distribution. Model 1 *a* was therefore used for the analysis of the $^{35}SO_4$ data. The least-squares estimates of the parameters are given in Table II for dogs 2, 3 and 4 and the corresponding curves for dog 2 are shown in Fig. 4 C. The parameter estimates for dogs 3 and 4 are influenced by the same uncertainty concerning evaporation as in the case of ^{131}I-albumin. The goodness of fit was acceptable for model 1 *a* but was not improved by using the more complex model 2 *a*, as can be seen in Fig. 4 D. The 95 % confidence region for the estimated parameters is shown in Fig. 5 B. From the values for dog 2 in Table II, it can be seen that k_{21} is larger than the corresponding value for I-albumin. Independent lymph-flow data can be used to estimate the volumes of the *functional* plasma and interstitial pools. The functional plasma volume, V_p, is of the same size, 42–54 ml, but the functional interstitial volume, V_I, is larger (5 ml, compared with 3.5 ml for the corresponding value for ^{131}I-albumin). It should be stressed that V_I here signifies the part of the interstitial compartment drained by the cannula. The estimates of pool volumes are also subject to large numerical errors.

Furthermore, it can also be concluded from the figures for dog 2 that the influx rate of $^{35}SO_4$ to plasma from the interstitial space approaches 100 % of the corresponding efflux rate from plasma.

^{24}Na

In this case, and also in the case of ^{42}K, the electrolyte was infused continuously, in order to maintain a constant plasma level. The reason for this was primarily to simplify the mathematical analysis (cf. 8); however, it was not possible to maintain the plasma level within $\pm 5\%$ (cf. 8) and, instead of analytical methods, numerical methods had to be used, with the advantage of accepting an arbitrary function for the plasma concentration of tracer.

The ^{24}Na data for dog 2 were invalidated for some unknown measuring and/or technical reason (see experimental results). The data from dogs 1, 3 and 4 were analysed. Using model 3 (cf. 9), the kinetic equations of which are

$$\frac{dC_2^*}{dt} = -(k_{12}+k_{42}+k_{02})\,C_2^*+k_{21}\,\frac{V_1}{V_2}\,C_1^*+k_{24}\,\frac{V_4}{V_2}\,C_4^* \quad (6)$$

$$\frac{dC_4^*}{dt} = -k_{24}\,C_4^*+k_{42}\,\frac{V_2}{V_4}\,C_2^* \quad (7)$$

a quite satisfactory fit was obtained, as illustrated for dog 1 in Fig. 4 E.

In this model the disappearance of the tracer from the interstitial fluids via the lymph system and other routes is described by a special rate constant (k_{02}). This parameter cannot be resolved (see eqs. (6) and (7)), but only estimated in addition to k_{12} (interstitium to plasma). Since the measured plasma concentration is used as a governing function, C_1^* (*t*), the other parameters k_{21} and V_1/V_2 can also only be estimated as the product $k_{21}(V_1/V_2)$.

The parameter estimates are given in Table III for dogs 1, 3 and 4 and the 95 % confidence region is shown in Fig. 5 C for dog 1. As can be seen from this figure, the parameters k_{42} and k_{24} are unreliably determined by the tracer data, and, in view of the apparent discrepancy of the conclusions about the concentration of stable Na in interstitial (C_I) and intracellular space (C_C) with common knowledge ($C_I \sim 14C_C$, cf. (28), (13)), model 3 is not an *adequate* model for the ^{24}Na data. By introducing the constraints $V_C \sim 4V_I$ (cf. 8) and $C_I \sim 14C_C$, i.e. $k_{24} = 3.5k_{42}$, it was also possible to fit the experimental tracer data, thus making model 3 compatible with these data. This model is, however, still not adequate, as can be seen from Fig. 5 D (see also Table III). The exchange between the interstitial and intracellular compartments (k_{24}, k_{42}) is also in this case unreliably determined, while the transcapillary ex-

Table III. *Parameter estimates for* ^{24}Na *using model 1b and 3 for the analysis of dogs 1, 3 and 4*

Parameters	Dog 1			Dog 3	Dog 4
	Model 1b	Model 3	Model 3 with constraints	Model 1b	Model 1b
$k_{21} \times V_1/V_2 (min^{-1})$	0.13	0.32	0.17	0.09	0.16
$k_{12} + k_{02} (min^{-1})$	0.14	0.34	0.18	0.11	0.17
$k_{42} (min^{-1})$	—	1.45	0.60	—	—
$k_{24} (min^{-1})$	—	1.05	2.10	—	—
T_{LAG} (min)	6	6	6	3	9
V_4/V_2	—	4 frozen	4 frozen	—	—
Derived quantities					
C_P/C_I	1.1	1.1	1.1	1.2	1.1
C_I/C_C	—	2.9	14 frozen	—	—

change (k_{21}, k_{12}) and interstitial outflow (k_{02}) remain reliably determined. In fact, even the simplest model 1b (see Fig. 3) is compatible with the tracer data and, according to Fig. 5E, the parameters $k_{02} + k_{12}$ and $k_{21}(V_1/V_2)$ are reliably determined.

^{42}K

A three-compartment system in series (model 3 in Fig. 3) was used in the analysis of the ^{42}K data.

This model differs from the open two-compartment model introduced by Conn & Robertson (8), and used by others (11, 15, 17, 29) in various respects. The plasma pool has not been considered as being infinite in size and has not been assumed to be in rapid exchange with the interstitial fluids, but has been described by an estimated "capillary plasma" forcing function.

The governing function C_1^* (the "capillary concentration") was estimated as a mean value of the concentrations in arterial plasma and cardiac lymph (coronary lymph ~ coronary venous plasma; cf. (11)). This approximation seems justified for all the ions studied in view of their rapid transcapillary exchange (cf. 30), but was only considered for potassium because of the approximation for this ion has the greatest influence (see Figs 4D, E and F).

The parameters $(k_{12} + k_{02})$, $(k_{21}(V_1/V_2))$, k_{24} and k_{42} were estimated by fitting C_2^* to the lymph-tracer data, with the assumption that these data were representative of the interstitial fluids. The ratio V_4/V_2 does not influence the C_2^* values, but only the values of the intra-cellular compartment. The least-squares estimates are given in Table IV for all the

Table IV. *Parameter estimates for* ^{42}K *using model 3 in the analysis of dogs 1, 2, 3 and 4*

Parameters	Dog 1	Dog 2	Dog 3	Dog 4
$k_{21} \times V_1/V_2 (min^{-1})$	0.16	0.045	0.03	0.11
$k_{12} + k_{02} (min^{-1})$	0.19	0.052	0.03	0.14
$k_{24} (min^{-1})$	1.38	0.194	0.22	0.17
$k_{42} (min^{-1})$	1.26	0.192	0.34	0.81
T_{LAG} (min)	0	6	3	9
Derived quantities				
C_P/C_I	1.2	1.2	1.0	1.3

dogs and the corresponding simulated curve C_2^* is shown in Fig. 4F for dog 2, compared with the experimental data. Model 3 was accepted as being compatible with the tracer data. The estimated parameter values are greatly dependent on the approximation of the "capillary concentration", as tested by repeating the calculations, using the primary plasma concentration values; the parameter values were then changed by factors ranging from 5 to 10.

The steady-state equation for the intra-cellular compartment is

$$\frac{C_C}{C_I} = \frac{k_{42}}{k_{24}} \frac{V_I}{V_C} \qquad (8)$$

Thus, in order to fulfil the constraint $C_C \sim 30C_I$ (cf. 13), the volume ratio V_I/V_C must be set equal to ~30 for dog 2. This is in conflict with common knowledge ($V_C \sim 4V_I$, cf. 8). As was found in the analysis of the ^{24}Na data, model 3 was not adequate, because of the large uncertainty in the estimated parameter values k_{24} and k_{42}. The same conclusion applies to model 3 for the description of the ^{42}K data, as can be seen from Fig. 5F, where the 95% confidence limits for the parameters k_{24} and k_{42} are shown for dog 2. An attempt to fit model 3 to the data of dog 2 with the constraints $C_C \sim 30C_I$ and $V_C \sim 4V_I$ did not produce an acceptable agreement with the experimental data.

By adding a fourth compartment in series (model 5 in Fig. 3), it is possible to fulfil the concentration and volume constraints; the steady-state equations for compartments 4 and 5 give the relations

$$V_2 = \frac{k_{24}}{k_{42}} \frac{C_4}{C_2} V_4 \qquad (9)$$

$$V_5 = \frac{k_{54}}{k_{45}} \frac{C_4}{C_5} V_4 \qquad (10)$$

With the assumptions that $C_4 = C_5 \sim 30 \, C_2$ and $V_4 + V_5 \sim 4 \, V_2$ it follows from the relations (9) and (10) that

$$1 + \frac{k_{54}}{k_{45}} = 120 \frac{k_{24}}{k_{42}} \qquad (11)$$

for example, for dog 2, where $k_{24} \sim k_{42}$, $k_{54} \sim 120 k_{45}$, $V_2 \sim 30 V_4$ and $V_5 \sim 120 V_4 \sim 4 V_2$.

A spectrum of possible solutions thus presents itself, the limits of which are determined by the uncertainty of the parameter estimates of k_{24} and k_{42} (see Fig. 7 F).

The introduction of a special lymph compartment (model 4 in Fig. 3) does not present any new, or simpler solution of the present problems. The uncertainty concerning the exchange on the cellular level remains.

DISCUSSION

The studies presented here show that several compartmental models for sodium and potassium exchange (model 3 and model 5) could easily be conformed so as to be compatible with the tracer data and it was also possible to make them consistent with independent relevant data from the literature. However, it was not possible to construct adequate models for the data, in the sense that the model parameters were reliably determined by the data. As the plots of the 95% confidence regions show (see Figs. 5C, D, F), the uncertainty in the rate constants between the interstitial and the intracellular compartments is too large to permit any far-reaching conclusions.

The tracer data only allowed for the estimation of transcapillary exchange for albumin and sulphate ions. The results so far are consistent concerning

(1) the slower exchange of albumin between plasma and interstitial fluids, compared with the corresponding values for the sulphate ion ($k = 0.0011 \pm 0.0002$ (2 S.D.) min^{-1} for I-albumin (dog 2) and $k = 0.0062 \pm 0.0002$ min^{-1} for SO$_4$ (dog 2)), and

(2) the influx rate of albumin and SO$_4$ to plasma (4–7% and ca. 100%, respectively, of the efflux rate from plasma).

The coefficient of transfer of albumin across the capillary walls was here estimated to be 0.0011 ± 0.0002 min^{-1} (dog 2), i.e. about 0.1% of the albumin in the plasma pool crossed the capillary walls each minute. This value is appreciably smaller than the values of 1–8% previously reported from a similar

study (2). The turnover time or the average time the albumin molecules spend in the interstitial space ($1/k_{02}$) was here estimated as 53 minutes for dog 2, a value which is also significantly smaller than the mean value of 257 minutes given by the same authors. The differences are due to the circumstance that these authors regarded the plasma pool as infinite, which was not the case in the present study (cf. page 173).

The barrier to potassium exchange has been claimed to be localized in the cell membrane by some authors (8, 11, 15, 29), while other authors (23, 30) have presented some evidence for its localization in the capillary wall. As pointed out above, our ^{42}K data do not allow any detailed conclusions about the exchange between interstitial and intracellular spaces, but the estimates of the rate constants, taking into account their large confidence limits (see Table IV and Fig. 5F), still suggest that the barrier is situated at the capillary wall. However, it should be noted that it was necessary to introduce one more compartment in series (see model 5 in Fig. 3 and the comments on page 178), in order to achieve compatibility with both ^{42}K tracer data and data from the literature concerning the concentration and distribution relations in interstitial and intracellular potassium spaces. Whether this auxiliary compartment should be interpreted as a second intracellular compartment (cf. 24, 29) or as a reflection of slow mixing in an inhomogeneous interstitial compartment (cf. 20), cannot be answered by this study. It is thus also impossible to localize more precisely the potassium-exchange barrier.

The analysis of ^{24}Na data presented similar problems to those discussed above for potassium (cf. also Sjöstrand (25)). The data could not resolve such complex models as discussed by Conn & Wood (9) for sodium exchange. In fact even the simplest two-compartment model (model 1 *b* in Fig. 3) was compatible with our data. No adequate model could be found for the transfer kinetics of this substance. The uncertainty of the rate constants connecting interstitial and intracellular compartments was too large (see Fig. 5D) and could not be reduced to a meaningful level by introducing the further constraints presented by literature data on the concentrations and distribution volumes of sodium (see Fig. 5D). However, the 95% confidence limits of these rate constants include the point estimates given for the same parameters by Conn & Wood (9) for a number of dogs.

In summary, it can be concluded that

1. experimental data of the type presented here

and previously used by other authors in the study of electrolyte kinetics in the dog's heart, cannot be described adequately in terms of a few distinct compartments; and

2. accordingly the same data, do not provide sufficient information for a reliable estimation of cellular exchange of sodium and potassium;

3. the transcapillary exchange of albumin and sulphate ions can be reliably estimated from the corresponding tracer data and compartmental models, which are adequate for these substances.

ACKNOWLEDGEMENTS

REFERENCES

1. Areskog, N.-H.: Some aspects of the hemodynamics of the heart-lung preparation of the dog. Acta Soc Med Upsal *67:* 143–152, 1962.
2. Areskog, N.-H., Arturson, G. & Grotte, G.: Studies on heart lymph. I. Kinetics of ^{131}I-albumin in dog heart-lung preparations. Acta physiol scand *62:* 209–217, 1964.
3. Arturson, G., Grotte, G., Malmberg, P., Samuelsson, R. & Sjöstrand, U.: Simultaneous measurements of myocardial lymph [42]K, [24]Na, [35]SO_4^{-2} and ^{131}I-Albumin concentration during steady-state infusion. In *Alfred Benzon Symposium II: Capillary permeability (Copenhagen, 1969),* pp. 319–323. Munksgaard, Copenhagen, 1970.
4. Beale, E. M. L.: Confidence regions in non-linear estimation. S R Stat Soc *22:* 41–76, 1960.
5. Benyon, P. R.: A review of numerical methods for digital simulation. Simulation *11:* 219–238, 1968.
6. Bill, A., Marsden, N. & Ulfendahl, H. R.: Some applications of a new gel filtration method for molecular separation. Scand J Lab Clin Invest *12:* 392–395, 1960.
7. Box, G. E. P.: Fitting empirical data. Ann NY Acad Sci *86:* 792–816, 1960.
8. Conn, H. L. & Robertson, J. S.: Kinetics of potassium transfer in the left ventricle of the intact dog. Amer J Physiol *181:* 319–324, 1955.
9. Conn, H. L. & Wood, J. C.: Sodium exchange and distribution in isolated heart of the normal dog. Amer J Physiol *197:* 631–636, 1959.
10. Danielson, B. G.: The distribution of some electrolytes in the heart. Acta physiol scand *62:* Suppl. 236, 1964.
11. Downey, H. F. & Kirk, E. S.: Coronary lymph: Specific activities in interstitial fluid during uptake of [42]K. Amer J Physiol *215:* 1177–1182, 1968.
12. Downey, H. F. & Kirk, E. S.: Indications from coronary lymph and early extraction data that steady-state uptake of [42]K is not primarily limited by the capillary wall. In *Alfred Benzon Symposium II: Capillary permeability.* Munksgaard, Copenhagen, 1970.

13. Folkow, B. & Neil, E.: *Circulation.* Oxford University Press, New York, 1971.
14. Gitlin, D.: Distribution dynamics of circulating and extravascular ^{131}I-plasma proteins. NY Acad Sci *70:* 122–136, 1957.
15. Grupp, G.: Potassium exchange in the dog heart in situ. Circul Res *13,* 279–289, 1963.
16. Langer, G. A.: Sodium exchange in dog ventricular muscle. Relation to frequency of contraction and its possible role in the control of myocardial contractility. J Gen Physiol *50:* 1221–1239, 1967.
17. Langer, G. A. & Brady, A. J.: Potassium in dog ventricular muscle: Kinetic studies of distribution and effects of varying frequency of contraction and potassium concentration of perfusate. Circul Res *18:* 164–177, 1966.
18. Lyttkens, L. & Sjöstrand, U.: *Dual-isotope determination by liquid scintillation spectrometry with special regard to samples with varying quenching.* Beckman Instruments International S. A., Geneva, 1971.
19. Östling, S. G.: Permeability of human red cells during hypotonic fractional mass hemolysis in dextran. Acta Univ Upsal *88:* 1970.
20. Page, E.: Cat heart muscle in vitro. III. The extracellular space. J Gen Physiol *46:* 201–213, 1962.
21. Page, E. & Solomon, A. K.: Cat heart muscle in vitro. I. Cell volumes and intracellular concentration in papillary muscle. J Gen Physiol *44:* 327–344, 1960.
22. Powell, M. J. D.: A method for minimizing a sum of squares of nonlinear functions without calculating derivatives. Computer Journal *7:* 303–307, 1965.
23. Renkin, E. M.: Transport of potassium-42 from blood to tissue in isolated mammalian skeletal muscles. Amer J Physiol *197:* 1205–1210, 1959.
24. Schreiber, S. S., Oratz, M. & Rothschild, M. A.: Ion diffusion delay in the beating mammalian heart. Proc Soc Exper Biol Med *116:* 164–167, 1964.
25. Sjöstrand, U.: Analysis of ionic tracer movements during single heart cycles. Acta physiol scand *61:* Suppl. 227, 1964.
26. Sjöstrand, U., Lyttkens, L., Öberg, P. Å. & Östling, S. G.: Spectrometry for determination of isotopic mixtures with special regard to biological and clinical investigations. Acta Soc Med Upsal *74:* 219–246, 1969.
27. Solomon, A. K.: Compartmental methods of kinetic analysis. In *Mineral metabolism.* Academic Press, New York, 1960.
28. Weidmann, S.: *Elektrophysiologie der Herzmuskelfaser.* H. Huber, Bern, 1956.
29. Wood, J. C. & Conn, H. L.: Potassium transfer kinetics in the isolated dog heart. Influence of contraction rate, ventricular fibrillation, high serum potassium and acetylcholine. Amer J Physiol *195:* 451–458, 1958.
30. Yudilevich, D. & Martin de Julian, P.: Potassium, sodium and iodide transcapillary exchange in the dog heart. Amer J Physiol *208:* 959–967, 1965.

Address for reprints:
Ulf Sjöstrand, M.D.
Department of Anaesthesiology & Intensive Care
Regional Hospital
S-701 85 Örebro
Sweden